EasyChair Preprint

№ 11881

Natural Circulation Flow Boiling Phenomenon Based on Cooler Temperature Variation Using FASSIP-04 Rectangular-TP Ver.2 Loop

Sunandi Kharisma, Dwi Yuliaji, Adhika Enggar Pamungkas, Arif Adtyas Budiman, Muhammad Rafel, Shendy Akbar Maryadi, Ryan Oktaviandi, Nur Rochman Budiyanto, Putut Hery Setiwan, Wayan Nata Septiadi and Mulya Juarsa

January 29, 2024

Natural Circulation Flow Boiling Phenomenon Based on Cooler Temperature Variation Using Rectangular-TP FASSIP-04 Ver.2 Loop

Sunandi Kharisma[1], Dwi Yuliaji[3,4], Adhika Enggar Pamungkas[2], Arif Adtyas Budiman[2], Muhammad Rafel[4], Shendy Akbar Maryadi[4], Ryan Oktaviandi[3], Nur Rochman Budiyanto[3], Putut Hery Setiyawan[2], Wayan Nata Septiadi[1], Mulya Juarsa[2,4,*]

[1]Heat Pipe and Nanotechnology Laboratory, Faculty of Engineering, Udayana University, Bukit Jimbaran, Badung, Bali, 80631, Indonesia.
{sunandikhar494}@gmail.com, {wayan.nata}@unud.ac.id
[2]Reactor Thermal-Fluids System Development Research Group (RTFSyDev), Center of Nuclear Reactor Technology and Safety, Research Organization of Nuclear Energy (ORTN), National Research and Innovation Agency of Indonesia (BRIN), Gd.80 KST. B.J. Habibie, Setu, Tangerang Selatan 15314, Banten, Indonesia.
{mulya.juarsa}@brin.go.id*
[3]Department of Mechanical and Industrial Engineering, Faculty of Engineering, Universitas Gadjah Mada, Jalan Grafika No 2 Kampus UGM, Yogyakarta 55281, Indonesia.
{ryanoktaviandi, nurrochmanbudiyanto1999 }@mail.ugm.ac.id
[4]Department of Mechanical Engineering, Faculty of Engineering and Science, Ibn Khaldun Bogor University, Jl. Sholeh Iskandar, RT.01/RW.10, Kedungbadak, Kota Bogor, Jawa Barat 16162, Indonesia.
{dwi.yuliaji}@uika-bogor.ac.id,
{akbarshendy, mrafel217}@gmail.com

Abstract. Passive cooling systems, which rely on the principle of natural circulation, commonly referred to as passive residual heat removal, can effectively dissipate the decay heat produced by nuclear reactors. Among these systems, the direct passive residual heat removal system is recognized as the most efficient. This study utilized the Loop Rectangular-TP FASSIP-04 Ver.2, operating on a direct heating model, to investigate the characteristics of two-phase natural circulation flow. The primary objective of this research was to gather data on temperature, flow rate, and flow regime characteristics observed during natural circulation. The experimental approach involved adjusting the cooling water temperature to 10°C, 15°C, and 20°C while maintaining a heating power of 5600 watts until reaching a steady-state condition. The findings of the study reveal that an increase in the cooling water temperature results in a more rapid attainment of steady-state conditions and a decrease in the average steady-state temperature. Specifically, the average steady-state temperatures changed to 97.77°C, 97.75°C, and 97.71°C, respectively. Furthermore, with the rise in cooling water temperature, the average Reynolds number increased from 5770 to 7027, indicating the transition to turbulent flow regime.

Keywords: Passive Cooling System, Natural Circulation, PRHR, oscillation, FASSIP-04 Ver.2

1 Introduction

The Fukushima Daiichi nuclear accident occurred on March 11, 2011, triggered by a 9.0 magnitude earthquake followed by a devastating tsunami. This catastrophe severely damaged the plant's cooling system, ultimately leading to a nuclear meltdown. The Fukushima Daiichi tragedy has been classified at the highest level (Level 7) on the International Atomic Energy Agency's (IAEA) disaster scale, indicating the release of substantial quantities of radioactive material with far-reaching health and environmental repercussions. The incident has sparked global concerns about the safety of nuclear power plants, raising doubts about their readiness for operation [1]. A Station Black Out (SBO) event unfolded at the Fukushima Daiichi Nuclear Power Plant (NPP) due to a non-functional power supply system, specifically the Emergency Diesel Generator (EDG). The EDG became submerged in seawater as tsunami waves exceeded 14 meters above the ground level within the NPP premises. Consequently, the active cooling system ceased to function entirely, posing a critical issue.

During this incident, the residual heat (decay heat) emanating from the reactor vessel could not be dissipated into the environment, primarily because the primary circulation pump remained inoperative [2]-[3]. As a consequence of a system failure leading to excessive heat buildup within the reactor core, the reactor core underwent a meltdown, causing damage to the reactor pressure vessel and the release of radiation into the environment [4]. The Fukushima Daiichi nuclear power plant accident, primarily affecting Units 1, 2, and 3 in Japan, served as a wake-up call for the nuclear industry, highlighting the necessity of preparedness for unforeseen events that surpass the design limits of existing nuclear power plants. Regardless of how diligently a power plant is operated and maintained, there remains the possibility of encountering unforeseen circumstances with potentially severe consequences. The Fukushima nuclear power plant accident can be classified as an "unknown to unknown" or multi-case event [5]. The Fukushima Daiichi accident yielded numerous valuable lessons in utilizing nuclear energy, spanning both technical and economic realms [6]. The accident has revealed several inherent design flaws and vulnerabilities, particularly when faced with unprecedented natural events.

The global nuclear community, including the IAEA, must learn from this incident and work on developing enhanced safety systems for nuclear power plants to prevent such accidents from occurring in the future [7]. Numerous advancements and ongoing research efforts in safety systems for nuclear power plants continue to progress, with a particular emphasis on cooling systems for nuclear reactors employing passive cooling methods based on the principles of natural circulation [8]-[9]. In the future, there is a growing consideration for implementing passive cooling systems that do not rely on electrical power inputs in the design of nuclear reactor safety systems [4]. Passive cooling systems, designed for the removal of nuclear reactor decay heat, commonly referred to as Passive Residual Heat Removal (PRHR), have been developed for various pressurized water reactor (PWR) and large-scale Boiling Water Reactor (BWR) nuclear power systems [10]. Its primary function is to dissipate decay heat from the reactor core by employing one or two fluid phases within the natural circulation circuit. This system is a mitigation measure in an accident or the SBO [11].

The most efficient PRHR system in use is the Direct Passive Residual Heat Removal (D-PRHR) system. D-PRHR is designed to dissipate decay heat from the primary system and can be connected to the top of the pressurizer as an inlet and directly to the reactor vessel. The SMART reactor exemplifies its application and is part of the Korea Atomic Energy Research Institute (KAERI) [12]. The D-PRHR system's inlet is positioned at the top of the pressurizer, and the return line from the condensate is connected to one of the injection nozzles on the reactor tube. Steam originating from the pressurizer travels into a heat exchanger in the tank's cooling section, where it condenses into water. The condensed steam is then reintroduced into the reactor tube via one of the direct injection nozzles. In addition to its application in the SMART Reactor, the D-PRHR system is also utilized in Russia's SG Passive Heat Removal System (WWER-640/V-407) and Mitsubishi Heavy Industries' Stand-alone Direct Heat Removal System (IMR), Ltd., in collaboration with Kyoto University, Central Research Institute of Electric Power Industry (CRIEPI), and Japan Atomic Power Company (JAPC) [12]–[16], among others. Because the D-PRHR system directly transfers heat to the primary reactor pipe system, which operates at high temperatures, the fluid within the natural circulation circuit undergoes a phase change. Specifically, it transitions from the liquid phase to the gas phase and condenses back into the liquid phase within the cooling tank.

Previous research conducted by [17] has explored the dynamics of bubbles, their collapse, and the impact of oscillating flows in natural circulation systems induced by boiling within the strands. This research provides insights into how the growth and clustering of bubbles in the Heating Section and the effect of bubble condensation under sub-cooled liquid conditions can accelerate the flow rate, leading to oscillations in natural circulation flow [18]. The presence of an insulated flow condition is regarded as unfavorable, especially when it comes to ensuring the stable extraction of heat from the reactor core. Therefore, it is imperative to investigate the conditions leading to oscillations and understand this phenomenon comprehensively.

In this study, the Rectangular-TP FASSIP-4 Ver.2 Loop experimental facility utilized the Direct system (D-PRHR), wherein the water in the strand comes into direct contact with the heat source and operates at a high-power setting until it reaches its boiling temperature. Under these conditions, the natural circulation flow rate becomes highly unstable, resulting in the NBO phenomenon. Given this context, the research will primarily focus on characterizing the temperature and natural circulation flow rate observed during the saturation conditions of the water working fluid before delving into further investigations concerning the NBO phenomenon. The research was conducted experimentally, involving variations in water temperature within the cooling section.

2 Experiments

2.1 Experimental Facilities

The experimental research facility uses Rectangular-TP FASSIP-04 Ver.2 Loop with the following specifications as shown in Table 1.

Table 1. Spesification of Rectangular-TP FASSIP-04 Ver.2 Loop

No	Description	Spesification
1	Material	*Stainless Steel* SS201
2	Outer diameter, D_{out}	25,4 mm
3	Inner diameter, D_{out}	23,4 mm
4	Width loop, L	1.320 mm
5	Height loop, H	6.000 mm
6	Total length loop, L_t	14.640 mm
7	Diameter ratio depends of total length loop, N_G	653,6
8	Volume working fluids	27,2 Liters

2.2 Experimental Setup

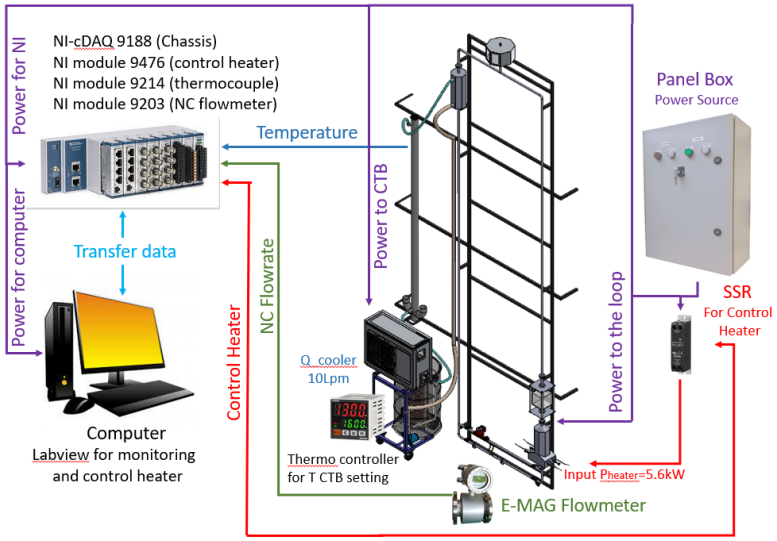

Fig. 1 Setup Experiment of Rectangular-TP FASSIP-04 Ver.2 Loop

The experiments conducted using the FASSIP-04 Rectangular-TP Ver.2 Loop were executed successfully, thanks to the excellent synchronization of the supporting apparatus. The experimental setup depicted in Fig. 1 above illustrates the interplay between these supporting apparatus components. The experiments were made possible by the electrical supply that powered various electronic devices essential for the experimental setup.

The panel box served as the power source for this setup, supplying power to several devices, including heaters, electromagnetic flowmeters, cooling systems, circulation pumps, NI-cDAQ 9188, and computer equipment. K-type thermocouples were employed as temperature sensors to measure the fluid's temperature within the FASSIP-04 Ver.2 Rectangular Loop. These thermocouples are responsible for measuring the fluid's temperature, and the readings are transmitted to the NI 9214 module via the NI cDAQ 9188 chassis, which is connected to a computer. This setup allows for the direct

monitoring of the fluid's temperature. For clarity and organization, each thermocouple sensor's placement on the FASSIP-04 Ver.02 Rectangular Loop with the National Instrument (NI) as the data logger corresponds to a specific port number on the NI 9214 Module, and each port is labeled according to the thermocouple sensor's position.

In addition to acquiring temperature data within the FASSIP-04 Ver.2 Rectangular Loop, fluid flow velocity data is also collected using an electromagnetic flowmeter sensor. The selection of an electromagnetic flowmeter allows for continuous and direct calculation of the circulating flow rate value on the FASSIP-04 Ver.2 Rectangular TP loop. The specific flowmeter utilized is the E-MAG Flowmeter brand, offering specifications outlined in Table 2. This choice was motivated by its exceptional accuracy and capacity to measure high-temperature flows. Furthermore, the flow rate data can be readily read and stored in the DAS-NI (Data Acquisition System-National Instruments).

Table. 1 Spesifcation of electromagnetic flow meter

Description	Spesifications
Brand	AUTOFLOW FLOWMETER
Model	E-MAG-1
Max Flow	8.8 m^3/hr
Power	AC 100-240V
Output	4 – 20 mA DC

2.3 Experimental Methods

The initial step before conducting the experiment involving the Rectangular Loop-TP FASSIP-04 Ver.2 is to undergo a series of tests and commissioning procedures. Once all pre-experimental processes have been completed, the experimental data collection can commence. The collected data is subjected to validation through scrutiny to identify any anomalies or disturbances that may have occurred during the experiment, ensuring the reliability and suitability of the data for analysis.

Upon confirming the correctness and appropriateness of the obtained data, the analysis phase begins. This involves examining data related to temperature variations, flow rates, and flow regimes throughout the experiment, as well as investigating the occurrence of the NBO phenomenon within the Rectangular-TP FASSIP-04 Ver.2 Loop. Conclusions are drawn from the analysis of this data based on the experimental results. The predetermined experimental matrix serves as a guideline throughout this process, as shown in Table 3.

Table. 2 Matrix experimental

Method	Heater Power [W]	Temperature WCT [°C]	Total Experiment
Experimental	5600W	10°C 15°C 20°C	3

3 Result

Experimental data collection was carried out continuously on the Rectangular Loop-TP FASSIP-04 Ver.2 by varying the coolant temperature to 10°C, 15°C, and 20°C, while maintaining the heater power setting in the heating tank at 5600 Watts. The temperature changes during the experiment were measured and recorded using the DAS-NI. The temperature measurement characteristics in the experiment are derived from the recorded temperature data obtained through the NI 9214 module. Additionally, data concerning the characteristics of natural circulation flow rates during the experiment were measured using a flowmeter. This data was continuously recorded to provide real-time flow rate values, which could be monitored directly using LabVIEW software. The flow rate change data was obtained based on the measurement instrument's recording from the NI 9203 module.

3.1 The Characteristic of Temperature

Temperature data collection during natural circulation experiments plays a crucial role in understanding the temporal evolution of temperatures within the loop. This data is instrumental in analyzing fluid flow behavior, heat transfer dynamics, and overall system efficiency. Recorded temperature data allows for the identification of trends, peak points, or other relevant conditions in the experiment. Moreover, temperature data serves as a foundation for calculating critical parameters, including the rate of temperature change within the natural circulation system under investigation. In essence, temperature data collection represents an essential step in gaining insight into and characterizing the performance of a natural circulation loop within experimental settings.

According to Fig. 2, the average ambient temperature is 26°C. It takes 4800 seconds to reach a steady state with a cooling temperature variation of 10°C. Once steady, the heater power is maintained for 16800 seconds. During this steady state, the water temperature within the HT averages 97.42°C, and the maximum temperature reached in the heating tank is 100.30°C

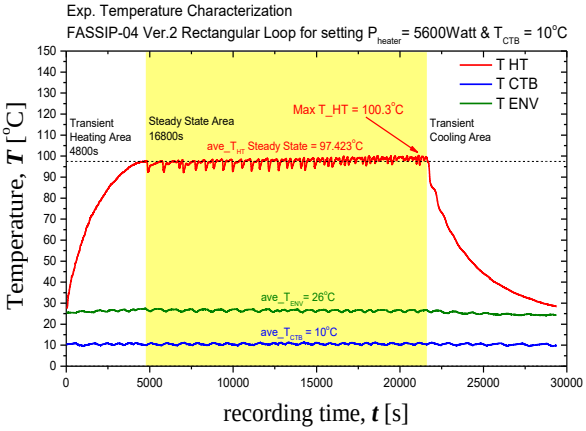

Fig. 2 Characteristic temperature of setting variation cooler 10°C

As per Fig. 3, the average ambient temperature is 27°C. It takes 4376 seconds to reach a steady state with a coolant temperature variation of 15°C. Once steady, the heater power is maintained for 18880 seconds. During this steady state, the water temperature within the HT averages 98.40°C, and the maximum temperature reached in the heating tank is 102.89°C.

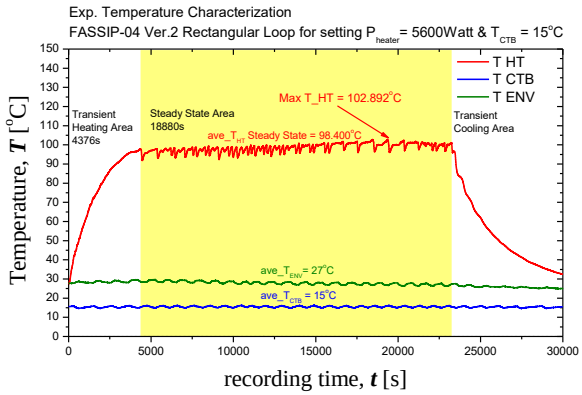

Fig. 3 Characteristic temperature of setting variation cooler 15°C

Based on Fig. 4, the average ambient temperature is 26°C, and the time needed to reach a steady state with a 20°C coolant temperature variation is 3539 seconds. Subsequently, at a steady state, the heater power is maintained for up to 18061 seconds. The water temperature that occurs in the heating tank at steady state for variations in the coolant temperature of 20°C averages 98.40°C, and the maximum temperature in the heating tank reaches 101.81°C.

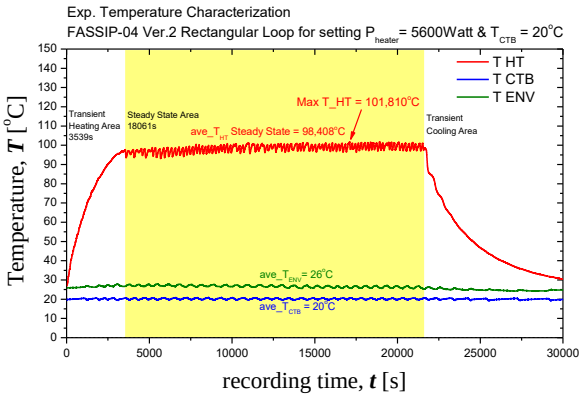

Fig. 4 Characteristic temperature of setting variation cooler 20°C

The results of the temperature characteristics reveal differences in the time it takes to reach different steady states for the three coolant temperature variations, namely 10°C, 15°C, and 20°C. These differences are summarized in Table 4.

Table 4. Interval transient heating time

Water temperature variation inside Cooling Tank [°C]	Transient heating time [s]
10	0s – 4800
15	0s - 4376
20	0s - 3539

Fig. 5 illustrates variations in coolant temperature settings, showcasing differences among the three variations: 10°C, 15°C, and 20°C. At 10°C coolant temperature setting, it takes 4800 seconds to reach a steady state condition, with a peak temperature of 97.77°C.

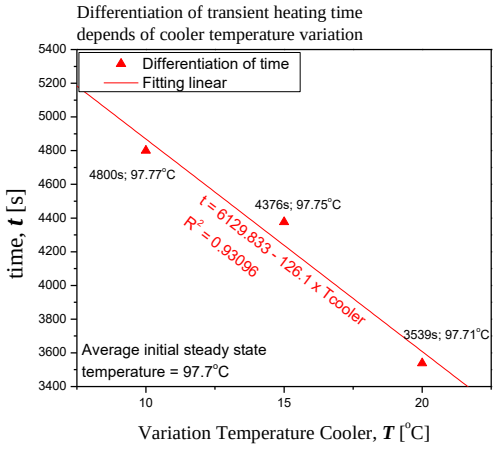

Fig. 5 Transient heating time depends of cooler temperature variation

Meanwhile, at the 15°C coolant temperature setting, the steady state is reached faster, in 4376 seconds, with a peak temperature of 97.75°C. Lastly, at the 20°C coolant temperature setting, it reaches a steady state even faster, in just 3539 seconds, with a temperature of 97.71°C. The graph in Fig. 5 shows that a coolant temperature variation of 20°C reaches a steady state more rapidly than variations of 10°C and 15°C. It is suggested that higher temperature settings on the cooler expedite the strand's attainment of a steady state condition. Furthermore, the graph demonstrates that the three variations follow a decreasing linear trend, allowing for linear fitting and the derivation of equations as follows.

$$t_{TH} = 6129.833 - 126.1\, T_{cooler} \quad (1)$$

Where t_{TH} is Transient Heating time (s) and T_{cooler} is Temperature setting cooler (°C)

Additionally, all three variations exhibit the same entry point into a steady state, specifically at a temperature of 97.7°C in the heating tank (HT). However, there are distinctions in the maximum values attained by the three coolant temperature variations, namely 10°C, 15°C, and 20°C. These differences are visually presented in the following Fig. 6.

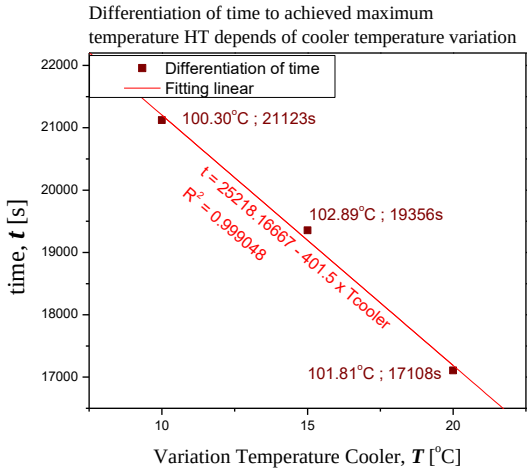

Fig. 6 Time to achieved maximum temperature HT depends of cooler temperature variation

The data presented in Fig. 6 provides compelling insights into the behavior of coolant temperature variations, precisely at 10°C, 15°C, and 20°C. Notably, the graph vividly demonstrates that when the coolant temperature variation is set at 20°C, the coolant rapidly ascends to its maximum temperature, outpacing the time required for variations at 10°C and 15°C. To elaborate, when the coolant temperature is set to 10°C, it takes 21123 seconds to attain its zenith, reaching a scorching 103.30°C. Meanwhile, when the temperature is maintained at 15°C, it reaches a peak of 102.89°C after 19356 seconds. Impressively, at a temperature variation of 20°C, the coolant reaches its maximum temperature of 101.81°C in a remarkably brief 17108 seconds.

The visual representation of the graph emphasizes that these three variations exhibit a consistent diminishing linear trend. This trend allows for the application of linear regression, yielding equations as follows, elucidating the relationship between temperature settings and the time required to reach maximum temperatures.

$$t_{Tmax} = 25218.16667 - 401.5\, T_{cooler} \tag{2}$$

Where t_{Tmax} is time for achieve maximum temperature heating tank (s) and T_{cooler} is Temperature setting cooler (°C)

3.2 The Characteristic of Natural Circulation Flow Rate

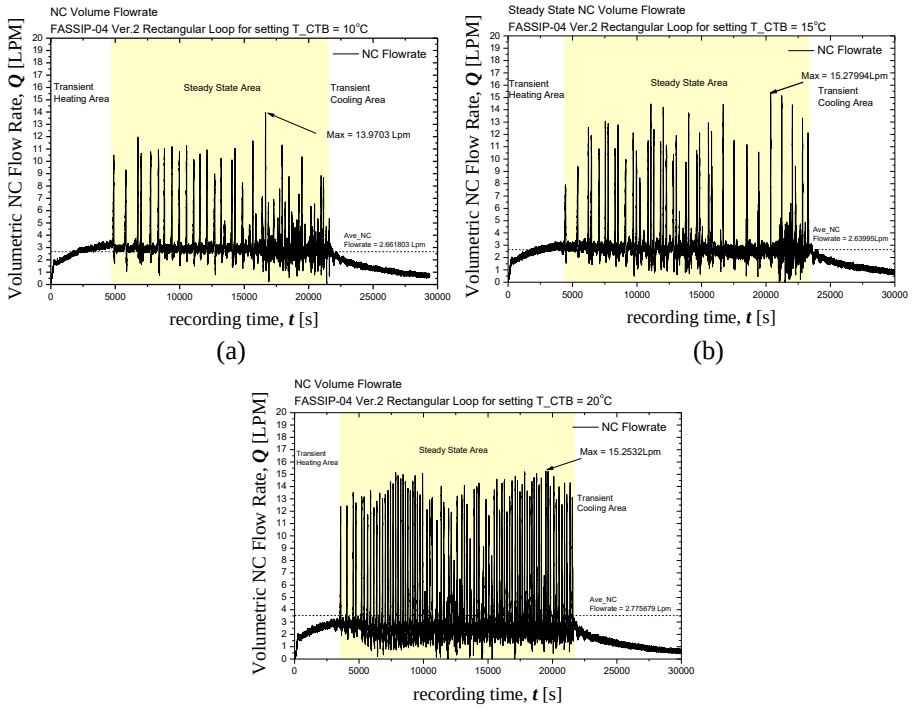

Fig. 7 Characteristic of NC Volume flowrate depends cooler variation

Based on Fig. 7(a), the natural circulation flow rate for the 10°C coolant variation gradually increases in sync with the rise in temperature in the heating tank (HT). The flow rate during natural circulation averages 2.66 LPM, with an initial transient heating stage lasting 4800 seconds and a steady-state period lasting 16800 seconds. During this steady state, the flow in the system experiences the NBO phenomenon, causing a significant increase in flow rate, reaching a maximum of 13.97 LPM.

In Fig. 7(b), the natural circulation flow rate for the 15°C coolant variation similarly increases alongside the rise in temperature at HT. The average flow rate during natural

circulation is 2.64 LPM, with an initial transient heating stage of 4376 seconds and a steady-state phase lasting 18880 seconds. During the steady state, the flow in the system encounters the NBO phenomenon, resulting in a high flow rate, reaching a maximum of 15.28 LPM.

Moving to Fig. 7(c), the natural circulation flow rate for the 20°C coolant variation also gradually increases with the rise in temperature at HT. The average flow rate during natural circulation is 2.77 LPM, with an initial transient heating stage of 3539 seconds and a steady-state phase lasting 18061 seconds. During this steady state, the flow experiences the NBO phenomenon, leading to a significant increase in flow rate, reaching a maximum of 15.25 LPM.

The results of the flow rate characteristics show differences in the maximum flow rate values that can be achieved at the three coolant temperature variations, namely 10°C, 15°C, and 20°C. These differences of volumetric natural circulation flow rate can be seen in Fig. 8.

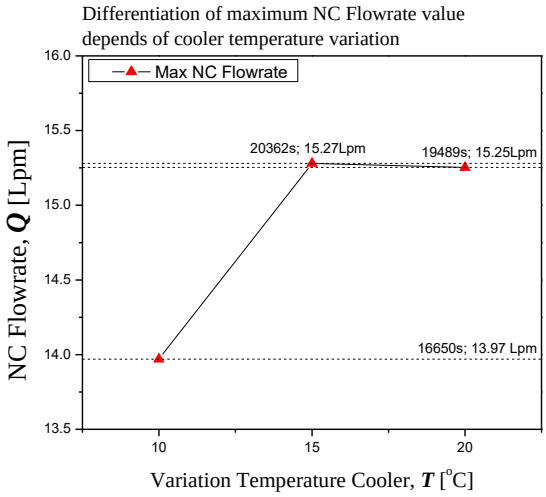

Fig. 8 Differentiation of maximum NC Flowrate value depends of cooler temperature variation

In Fig. 8, it is evident that with a variation of 10°C, the natural circulation flow rate reaches its peak at 13.97 LPM around 16650 seconds. With a 15°C variation, this flow rate increases to 15.27 LPM at approximately 20362 seconds. However, with a 20°C variation, the flow rate in the loop decreases to 15.25 LPM at approximately 19489 seconds. As the coolant temperature variation increases, it can be observed that the maximum temperature achievable within the loop also varies.

The graph in Fig. 8 reveals a clear trend regarding the natural circulation flow rate in relation to different coolant temperature variations. For the 10°C variation, the flow rate gradually increases, eventually reaching its peak at 13.97 LPM around 16650 seconds into the experiment. When the coolant temperature is raised by 15°C, the flow rate exhibits a further increase, reaching a maximum of 15.27 LPM at approximately 20362 seconds. However, an interesting shift occurs when the coolant temperature variation is set at 20°C. In this case, the flow rate in the loop follows a slightly different trajectory.

It initially rises but eventually starts to decline, settling at 15.25 LPM around 19489 seconds. This variation in natural circulation flow rates highlights the influence of coolant temperature on the thermal behavior of the system. Additionally, it's worth noting that as the coolant temperature variation increases, the maximum attainable temperature within the loop undergoes corresponding adjustments.

3.3 Natural Circulation Flow Regime

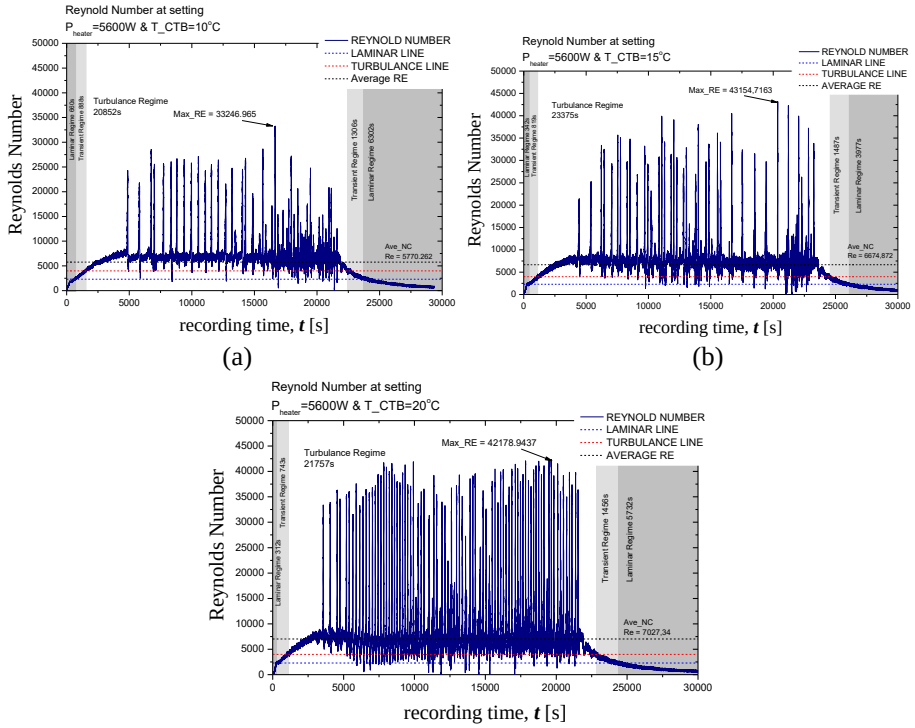

Fig. 9 Reynolds number characteristic depends of setting cooler temperature

In Fig. 9(a), with a power setting of 5600W and a 10°C coolant temperature variation, the Reynolds Number demonstrates characteristics of a turbulent flow regime. The average Reynolds Number during natural circulation flow is calculated at 5770.262. The flow regime undergoes a transition from laminar at 0s to 660s, enters the transient flow regime at 888s, and eventually shifts to a turbulent state at 20852s. Throughout the steady state conditions, the flow remains turbulent and experiences the NBO phenomenon, resulting in a substantial increase in the flow rate value. This increase is mirrored by the Reynolds Number, which reaches its maximum value of 33246.965.

Moving on to Fig. 9(b), the Reynolds Number also displays characteristics of a turbulent flow regime at the same power setting of 5600W but with a coolant temperature variation of 15°C. The average Reynolds Number throughout natural circulation flow

is calculated at 6674.872. The flow regime experiences a transition from laminar at 0s to 342s, enters the transient flow regime at 819s, and shifts to a turbulent state at 23375s. During steady-state conditions, the flow remains turbulent and experiences the NBO phenomenon, leading to a significant increase in the flow rate value. This increase is reflected in the Reynolds Number, which reaches its maximum value of 43154.716.

Finally, in Fig. 9(c), under the same power setting of 5600W and a coolant temperature variation of 20°C, the Reynolds Number also exhibits characteristics of a turbulent flow regime. The average Reynolds Number during natural circulation flow is determined to be 7027.34. The flow regime transitions from laminar at 0s to 312s, enters the transient flow regime at 743s, and becomes turbulent at 21757s. During steady-state conditions, the flow remains turbulent and experiences the NBO phenomenon, resulting in a substantial increase in the flow rate value. This increase is mirrored by the Reynolds Number, which reaches its maximum value of 42178.943.

The results of the flow regime characteristics show that there are differences in the average Reynolds Number achieved at the three coolant temperature variations, namely 10°C, 15°C, and 20°C. These differences can be seen in the following Fig. 10.

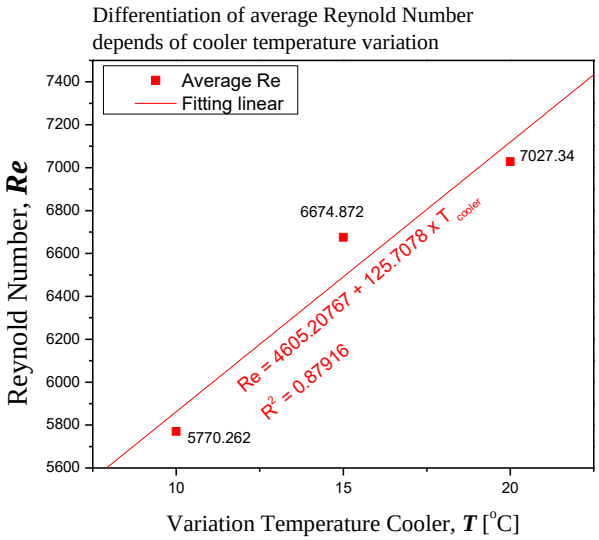

Fig. 10 Average Reynold number depends of cooler temperature variation

Based on the data in Fig 10, we can conclude that the 10°C coolant temperature variation results in the lowest average Reynolds Number compared to the 15°C and 20°C variations. This suggests that as the cooler temperature setting increases, the average Reynolds Number on the strand also increases. Furthermore, the data for these three variations form a linear graph with an ascending trend, which can be linearly fitted to yield the following equation (3).

$$Re_{ave} = 4605.20767 + 125.7078\, T_{cooler} \tag{3}$$

Where Re_{ave} is Average value of Reynolds Number (s), and T_{cooler} is Temperature setting of cooler (^{o}C)

4 Conclusion

The analysis of temperature data provides valuable insights into the behavior of the system across three different coolant temperature settings. Notably, it becomes evident that a higher temperature setting on the cooler leads to a faster attainment of a steady-state condition within the loop. This suggests that the thermal equilibrium of the system is achieved more rapidly when the coolant temperature is set at a higher level. Additionally, the temperature data also reveals a relationship between the temperature setting on the cooler and the rate at which the working fluid within the system reaches its maximum temperature. When the cooler temperature setting is elevated, the working fluid tends to heat up more rapidly, further emphasizing the influence of temperature control on system dynamics.

Shifting our focus to the natural circulation flow rates, it is apparent that as the value of the coolant temperature variation increases, so does the maximum flow rate achievable within the loop. This trend suggests that variations in coolant temperature have a direct impact on the flow dynamics of the system, with higher temperature variations resulting in greater flow rates. It shows that increasing the cooling water causes steady-state conditions to be reached more quickly and a decrease in the average steady-state temperature, respectively, changing from 97.77°C, 97.75°C, and 97.71°C.

Finally, when we delve into the analysis of flow regime characteristics, a clear pattern emerges. The coolant temperature variation of 10°C stands out with the smallest average Reynolds Number when compared to the variations of 15°C and 20°C. This observation underscores the relationship between the temperature setting on the cooler and the average Reynolds Number within the loop. Specifically, higher cooler temperature settings correspond to higher average Reynolds Numbers, indicating a shift towards a more turbulent flow regime as the temperature increases. This insight provides valuable information about the flow behavior within the system under different temperature conditions. In addition, the average Reynolds number increases as the cooling water temperature rises from 5770 to 7027, which enters the turbulent flow regime.

5 Acknowledge

The Program of “Riset Inovasi untuk Indonesia Maju” (RIIM) batch-1 LPDP Mandatori BRIN funded this research with contract number B-811/II.7.5/FR/6/2022 and B-2103/III.2/HK.04.03/7/2022 for the 2022-2023 fiscal year. Thanks to the Head of Research Center for Nuclear Reactor Technology (PRTRN) BATAN BRIN for his support. Also, thanks to the RTFSyDev. Research groups colleagues for their involvement in these research activities.

6 References

[1] IAEA TECDOC 1624, “Passive Safety Systems and Natural Circulation in Water Cooled Nuclear Power Plants,” Vienna, Nov. 2009.

[2] Y. S. Kim, S. W. Bae, S. Cho, K. H. Kang, and H. S. Park, “Application of direct passive residual heat removal system to the SMART reactor,” *Ann Nucl Energy*, vol. 89, pp. 56–62, Mar. 2016, doi: 10.1016/j.anucene.2015.11.025.

[3] Y. J. Chung, S. H. Yang, H. C. Kim, and S. Q. Zee, “Thermal hydraulic calculation in a passive residual heat removal system of the SMART-P plant for forced and natural convection conditions,” *Nuclear Engineering and Design*, vol. 232, no. 3. pp. 277–288, Aug. 2004. doi: 10.1016/j.nucengdes.2004.07.002.

[4] R. Gauntt *et al.*, “SANDIA REPORT Fukushima Daiichi Accident Study (Status as of April 2012).” [Online]. Available: http://www.ntis.gov/help/ordermethods.asp?loc=7-4-0#online

[5] A. R. Antariksawan, S. Widodo, M. Juarsa, D. Haryanto, M. H. Kusuma, and N. Putra, “Numerical study on natural circulation characteristics in FASSIP-02 experimental facility using RELAP5 code,” in *IOP Conference Series: Earth and Environmental Science*, Institute of Physics Publishing, Jan. 2018. doi: 10.1088/1755-1315/105/1/012090.

[6] A. Adtyas Budiman, G. B. Heru, M. Juarsa, P. Teknologi dan Keselamatan Reaktor Nuklir-BATAN, and R. Artikel, “Jurnal Pengembangan Energi Nuklir Analisis Sistem Pengendalian Temperatur WHT dalam Operasi Tunak Untai Uji FASSIP-02 INFORMASI ARTIKEL ABSTRAK,” 2019.

[7] M. Juarsa, A. R. Antariksawan, M. H. Kusuma, D. Haryanto, and N. Putra, “Estimation of natural circulation flow based on temperature in the FASSIP-02 large-scale test loop facility,” in *IOP Conference Series: Earth and Environmental Science*, Institute of Physics Publishing, Jan. 2018. doi: 10.1088/1755-1315/105/1/012091.

[8] “The Fukushima Nuclear Accident and Crisis Management-Lessons for Japan-U.S. Alliance Cooperation.”

[9] R. Gauntt *et al.*, “SANDIA REPORT Fukushima Daiichi Accident Study (Status as of April 2012).” [Online]. Available: http://www.ntis.gov/help/ordermethods.asp?loc=7-4-0#online

[10] IAEA TECDOC Series 1785, “Design Safety Considerations for Water Cooled Small Modular Reactors Incorporating Lessons Learned from the Fukushima Daiichi Accident,” VIenna, 2016.

[11] Dr. A. R. Antariksawan, S. Widodo, M. Juarsa, D. Haryanto, M. H. Kusuma, and N. Putra, “SIMULATION OF OPERATIONAL CONDITIONS OF FASSIP-02 NATURAL CIRCULATION COOLING SYSTEM EXPERIMENTAL LOOP,” *Jurnal Sains dan Teknologi Nuklir Indonesia*, vol. 19, no. 1, p. 40, Feb. 2018, doi: 10.17146/jstni.2018.19.1.4036.

[12] P. K. Vijayan, M. Sharma, and D. Saha, “Steady state and stability characteristics of single-phase natural circulation in a rectangular loop with different

heater and cooler orientations," *Exp Therm Fluid Sci*, vol. 31, no. 8, pp. 925–945, Aug. 2007, doi: 10.1016/j.expthermflusci.2006.10.003.

[13] D. C. Sun *et al.*, "Experimental investigation on natural circulation characteristics of emergency passive residual heat removal system in HPR1000," *Progress in Nuclear Energy*, vol. 103, pp. 1–7, Mar. 2018, doi: 10.1016/j.pnucene.2017.11.001.

[14] K. Hibi, H. Ono, and T. Kanagawa, "Integrated modular water reactor (IMR) design," in *Nuclear Engineering and Design*, May 2004, pp. 253–266. doi: 10.1016/j.nucengdes.2003.11.025.

[15] Y. A. Kurakov, Y. G. Dragunov, A. K. Podshibiakin, N. S. Fil, S. A. Logvinov, and Y. K. Sitnik, "Development and validation of natural circulation based systems for new WWER designs."

[16] B. Zohuri, "Direct Reactor Auxiliary Cooling System," in *Heat Pipe Applications in Fission Driven Nuclear Power Plants*, Springer International Publishing, 2019, pp. 203–218. doi: 10.1007/978-3-030-05882-1_7.

[17] T. Ishida, T. Kusunokl, N. Odano, N. Nakajima, and M. Ocfflai, "IAEA-SR-218/20 DESIGN OF PASSIVELY SAFE SMALL REACTOR FOR DISTRIBUTED ENERGY SYSTEM AND TECHNOLOGY DEVELOPMENT."

[18] J. Naik L, J. Bhati, S. Paruya, and G. M. Shahurao, "Onset of Flow Oscillation in a Natural Circulation Boiling Loop - Role of Bubble Dynamics," *Ind Eng Chem Res*, vol. 60, no. 2, pp. 955–968, Jan. 2021, doi: 10.1021/acs.iecr.0c04179.

[19] P. Brahmanda Sudarsana, W. Nata Septiadi, and M. Juarsa, "Jurnal Pengembangan Energi Nuklir Kajian Performa Passive Residual Heat Removal System (PRHRS) pada System-Integrated Advanced Modular Reactor (SMART) INFORMASI ARTIKEL ABSTRAK," 2021.